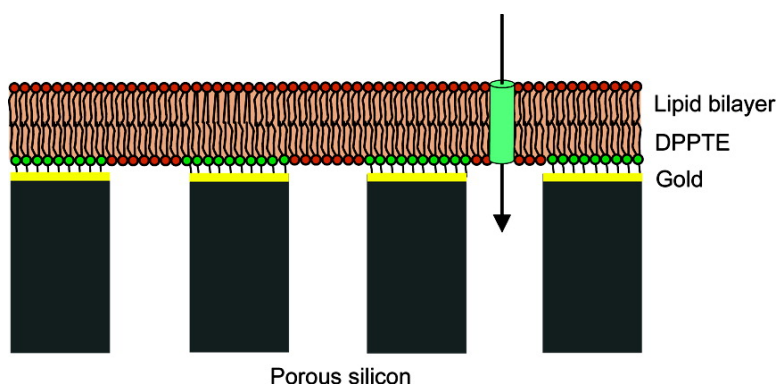


## Channel Activity of a Viral Transmembrane Peptide in Micro-BLMs: Vpu from HIV-1

Winfried Rmer, Yuen H. Lam, Dahlia Fischer, Anthony Watts, Wolfgang B. Fischer, Petra Gring, Ralf B. Wehrspohn, Ulrich Gsele, and Claudia Steinem

*J. Am. Chem. Soc.*, **2004**, 126 (49), 16267-16274 • DOI: 10.1021/ja0451970 • Publication Date (Web): 13 November 2004

Downloaded from <http://pubs.acs.org> on April 5, 2009



### More About This Article

Additional resources and features associated with this article are available within the HTML version:

- Supporting Information
- Links to the 4 articles that cite this article, as of the time of this article download
- Access to high resolution figures
- Links to articles and content related to this article
- Copyright permission to reproduce figures and/or text from this article

[View the Full Text HTML](#)

## Channel Activity of a Viral Transmembrane Peptide in Micro-BLMs: Vpu<sub>1–32</sub> from HIV-1

Winfried Römer,<sup>†</sup> Yuen H. Lam,<sup>‡</sup> Dahlia Fischer,<sup>‡,§</sup> Anthony Watts,<sup>‡</sup>  
Wolfgang B. Fischer,<sup>‡,⊥</sup> Petra Göring,<sup>||</sup> Ralf B. Wehrspohn,<sup>||,¶</sup> Ulrich Gösele,<sup>||</sup> and  
Claudia Steinem<sup>\*,†</sup>

Contribution from the Institut für Analytische Chemie, Chemo- und Biosensorik, Universität Regensburg, 93040 Regensburg, Germany, Department of Biochemistry, Biomembrane Structure Unit, University of Oxford, Oxford, OX1 3QU, U.K., and Max-Planck-Institut für Mikrostrukturphysik, 06120 Halle, Germany

Received August 9, 2004; E-mail: claudia.steinem@chemie.uni-regensburg.de

**Abstract:** We report for the first time on pore-suspending lipid bilayers, which we call micro-black lipid membranes (micro-BLMs), based on a highly ordered macroporous silicon array. Micro-BLMs were established by first functionalizing the backside porous silicon surface with gold and then chemisorbing 1,2-dipalmitoyl-*sn*-glycero-3-phosphothioethanol followed by spreading 1,2-diphytanoyl-*sn*-glycero-3-phosphocholine dissolved in *n*-decane. Impedance spectroscopy revealed the formation of single lipid bilayers confirmed by a mean specific capacitance of  $0.6 \pm 0.2 \mu\text{F}/\text{cm}^2$ . Membrane resistances were in the GΩ-regime and beyond. The potential of the system for single channel recordings was demonstrated by inserting the transmembrane domain of the HIV-1 accessory peptide Vpu<sub>1–32</sub>, which forms helix bundles with characteristic opening states. We elucidated different amilorides as potential drugs to inhibit channel activity of Vpu.

### Introduction

Ion channels play key roles in the function of living cells, and as a consequence, there are many potential drug targets among them. Two main techniques are used to investigate ion channel activity: patch clamp experiments and recordings on planar lipid bilayers (black lipid membranes, BLMs), both allowing the study of ion channel behavior by recording the transmembrane current caused by opening and closing of the channels. From these recordings, single channel conductance as well as opening and closing probabilities can be deduced. While patch clamp experiments start from native membranes, planar bilayers are formed across apertures in thin films, often Teflon of 5 to 25 μm with hole diameters of 0.1–1 mm,<sup>1–4</sup> with the advantage that the composition of the lipid membrane and the surrounding electrolyte solution on both sides of the membrane can be defined precisely. In particular, these planar lipid bilayers have been reassessed in recent years since ion

channels have been identified as major drug targets.<sup>5</sup> However classical BLMs, based on small apertures in thin Teflon films, are not suited for automation and miniaturization as required for biosensors and high-throughput screening assays for potential drugs. Thus, new strategies based on microfabricated apertures in silicon<sup>6</sup> and glass<sup>7,8</sup> have been recently developed, which allow for rather small apertures of 0.7 μm to a few millimeters<sup>6,7</sup> to be generated. Lipid membranes suspended across 0.7–100 μm apertures have been prepared with various techniques ranging from depositing lipids in an organic solvent to spreading of a giant unilamellar vesicle.<sup>9–13</sup> The long-term stability of these membranes is merely on the order of up to several hours. For biosensor applications, however, a long-term stability of several days is desirable. So far, this can only be achieved by solid support membranes,<sup>14–17</sup> which enable the rational design

<sup>†</sup> Universität Regensburg.

<sup>‡</sup> University of Oxford.

<sup>§</sup>Current address: Institut für Organische Chemie, Universität Karlsruhe (TH), 76131 Karlsruhe, Germany.

<sup>⊥</sup>Current address: Bionanotechnology IRC, Clarendon Laboratory, Department of Physics, University of Oxford, Oxford OX1 3PU, UK.

<sup>||</sup>Max-Planck-Institut für Mikrostrukturphysik.

<sup>¶</sup>Current address: Department Physik, Universität Paderborn, 33095 Paderborn, Germany.

- (1) Mueller, P.; Rudin, D. O.; Tien, H. T.; Wescott, W. C. *J. Phys. Chem.* **1963**, *67*, 534–535.
- (2) Tien, H. T.; Ottova, A. L. *Membrane biophysics: planar lipid bilayers and spherical liposomes*; Elsevier: Amsterdam, 2000.
- (3) Montal, M. *Methods Enzymol.* **1974**, *32*, 545–554.
- (4) Montal, M.; Mueller, P. *Proc. Natl. Acad. Sci. U.S.A.* **1972**, *69*, 3561–3566.

- (5) Drews, J. *Science* **2000**, *287*, 1960–1964.
- (6) Pantoja, R.; Sigg, D.; Blunck, R.; Bezanilla, F.; Heath, J. R. *Biophys. J.* **2001**, *81*, 2389–2394.
- (7) Fertig, N.; Meyer, C.; Blick, R. H.; Trautmann, C.; Behrends, J. C. *Phys. Rev. E* **2001**, *64*, 040901–040904.
- (8) Fertig, N.; Georg, M.; Klau, M.; Meyer, C.; Tilke, A.; Sobotta, C.; Blick, R.; Behrends, J. C. *Recept. Channels* **2003**, *9*, 29–40.
- (9) Schmidt, C.; Mayer, M.; Vogel, H. *Angew. Chem., Int. Ed.* **2000**, *39*, 3137–3140.
- (10) Ogier, S. D.; Bushby, R. J.; Cheng, Y.; Evans, S. D.; Evans, S. W.; Jenkins, T. A.; Knowles, P. F.; Miles, R. E. *Langmuir* **2000**, *16*, 5696–5701.
- (11) Osborn, T. D.; Yager, P. *Langmuir* **1995**, *11*, 8–12.
- (12) Cheng, Y.; Bushby, R. J.; Evans, S. D.; Knowles, P. F.; Miles, R. E.; Ogier, S. D. *Langmuir* **2001**, *17*, 1240–1242.
- (13) Peterman, M. C.; Ziebarth, J. M.; Braha, O.; Bayley, H.; Fishman, H. A.; Bloom, D. M. *Biomed. Microdevices* **2002**, *4*, 231–236.
- (14) Purucker, O.; Hillebrandt, H.; Adlkofer, K.; Tanaka, M. *Electrochim. Acta* **2001**, *47*, 791–798.
- (15) Steinem, C.; Janshoff, A.; Ulrich, W.-P.; Sieber, M.; Galla, H.-J. *Biochim. Biophys. Acta* **1996**, *1279*, 169–180.

of biosensor devices for high-throughput screening based on sophisticated micromachined chip technology. However, these membranes are not suited for single channel recordings, since first, the interface capacitance abolishes a continuous ion flow, and second, a  $G\Omega$  seal between the bilayer and the support is hardly achieved. Moreover, solution exchange is not feasible since there is only a 1–5 nm water film that separates the bilayer from the support.

With the aim to combine the merits of both membrane systems, free-standing planar lipid bilayers and solid-supported membranes, we used macroporous silicon substrates with pore sizes of 1  $\mu\text{m}$  that were covered with a lipid bilayer. In this hybrid membrane system, the membrane-suspended pores act as planar lipid bilayers, while the membranes attached to the pore rims provide mechanical stability as obtained for solid-supported membranes.

To elucidate the potential of this membrane type for investigating channel activity, a potential drug target for HIV treatment, Vpu, was investigated. Vpu is a small 81 amino acid integral membrane protein that forms cation-selective ion channels that is encoded by the human immunodeficiency virus type 1 (HIV-1).<sup>18–20</sup> Vpu comprises a highly hydrophobic N-terminal helical transmembrane (TM) domain encompassing residues 8–25 and a large hydrophilic phosphorylated cytoplasmatic C-terminal domain.<sup>19,21–24</sup> These two distinct structural domains of Vpu exhibit independent functionalities: while the latter domain is involved in the degradation of the virus receptor CD4 in the endoplasmic reticulum, the former domain enhances viral release/secretion from the cell surface.<sup>21,22</sup> Reconstitution of synthetic Vpu fragments in lipid bilayers identified ion channel activity for a sequence corresponding to the helical TM domain of Vpu, forming a water-filled bundle of homooligomers of an undetermined number of subunits in membranes.<sup>22,25,26</sup> Recent studies show that the cytoplasmatic domain encompassing two shorter amphipathic in-plane helices<sup>23,26</sup> regulates the lifetime of the TM channel in the conductive state.<sup>26</sup> Amiloride derivatives have been shown to block channel activity and the enhancement of virus-like particle budding caused by Vpu and might thus be identified as potential antagonists.

## Results

### Characterization of the Macroporous Silicon Substrate.

Scanning electron microscopy (SEM) images of the front and backside as well as side views of macroporous silicon, prepared by photoelectrochemical etching,<sup>27</sup> were taken. SEM images of the front side (Figure 1a) after the anodization procedure show

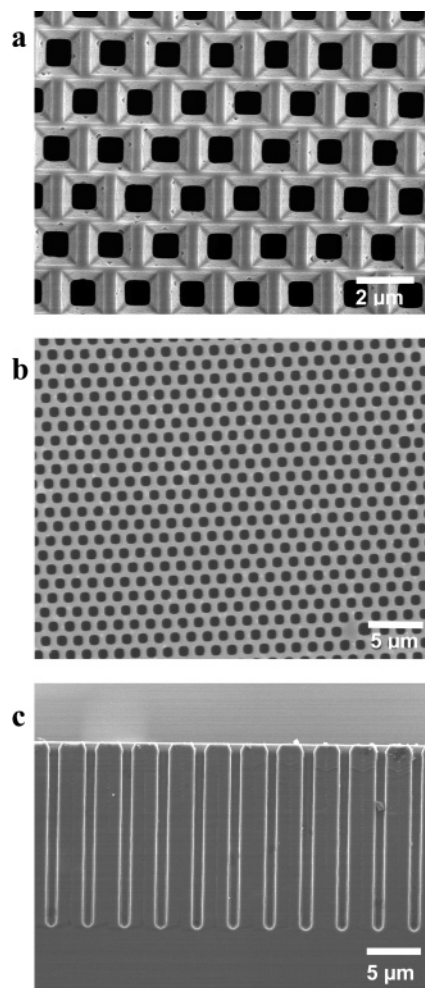


**Figure 1.** Scanning electron microscopy (SEM) micrographs of hexagonally ordered macroporous silicon substrates covered with a gold layer. SEM images of (a) front, (b) bottom, and (c) side view are presented. Photoelectrochemical etching was conducted in 4 wt % hydrofluoric acid at  $T = 10\text{ }^{\circ}\text{C}$  and  $V = 2.7\text{ V}$ . The pore diameter was  $1.0 \pm 0.1\text{ }\mu\text{m}$  with a surface porosity of  $22 \pm 3\%$  calculated by pixel analysis.

square-shaped pores with an etch length of around 1.0–1.2  $\mu\text{m}$ . The backside of the macroporous silicon substrate (Figure 1b) exhibits pores with diameters of  $1.0 \pm 0.1\text{ }\mu\text{m}$ . In contrast to the initial square-shaped photolithographically formed pore nuclei at the front side of the silicon wafer, the opened pores at the backside are circular and almost perfectly hexagonally ordered. Only very few defects are present. A surface porosity of  $22 \pm 3\%$  was calculated by pixel analysis from the SEM images. A side view of a macroporous silicon substrate, where the backside of the pores has not yet been removed (Figure 1c), reveals that the pores grow perpendicular to the substrate surface. This almost perfect growth of each individual pore is a consequence not only of the lithographic pattern but also of the orientation of the silicon single crystal. Each pore grows with the same velocity, and thus, the thickness of the porous substrate is determined by the anodization time. Typically, a thickness of 50–200  $\mu\text{m}$  is adjusted to ensure mechanical stability.

By means of impedance spectroscopy, the electrochemical characteristics of porous silicon substrates open to the electrolyte on both sides were investigated. Only an ohmic resistance of the electrolyte was detected with a small contribution from the platinum electrodes at frequencies below 1 Hz (see Supporting

- (16) Tien, H. T.; Ottova, A. L. *Electrochim. Acta* **1998**, *43*, 3587–3610.  
 (17) Sackmann, E. *Science* **1996**, *271*, 43–48.  
 (18) Marassi, F. M.; Ma, C.; Gratkowski, H.; Straus, S. K.; Strelbe, K.; Oblatt-Montal, M.; Montal, M.; Opella, S. J. *Proc. Natl. Acad. Sci. U.S.A.* **1999**, *96*, 14336–14341.  
 (19) Fischer, W. B. *FEBS Lett.* **2003**, *552*, 39–46.  
 (20) Kochendoerfer, G. G.; Jones, D. H.; Lee, S.; Oblatt-Montal, M.; Opella, S. J.; Montal, M. *J. Am. Chem. Soc.* **2004**, *126*, 2439–2446.  
 (21) Schubert, U.; Ferrer-Montiel, A. V.; Oblatt-Montal, M.; Henklein, P.; Strelbe, K.; Montal, M. *FEBS Lett.* **1996**, *398*, 12–18.  
 (22) Ewart, G. D.; Mills, K.; Cox, G. B.; Gage, P. W. *Eur. Biophys. J.* **2002**, *31*, 26–35.  
 (23) Park, S. H.; Mrse, A. A.; Nevzorov, A. A.; Mesleh, M. F.; Oblatt-Montal, M.; Montal, M.; Opella, S. J. *J. Mol. Biol.* **2003**, *333*, 409–424.  
 (24) Ewart, G. D.; Sutherland, T.; Gage, P. W.; Cox, G. B. *J. Virol.* **1996**, *70*, 7108–7115.  
 (25) Lamb, R. A.; Pinto, L. H. *Virology* **1997**, *229*, 1–11.  
 (26) Montal, M. *FEBS Lett.* **2003**, *552*, 47–53.  
 (27) Lehmann, V. *Electrochemistry of silicon*; Wiley-VCH Verlag GmbH: Weinheim, 2002.

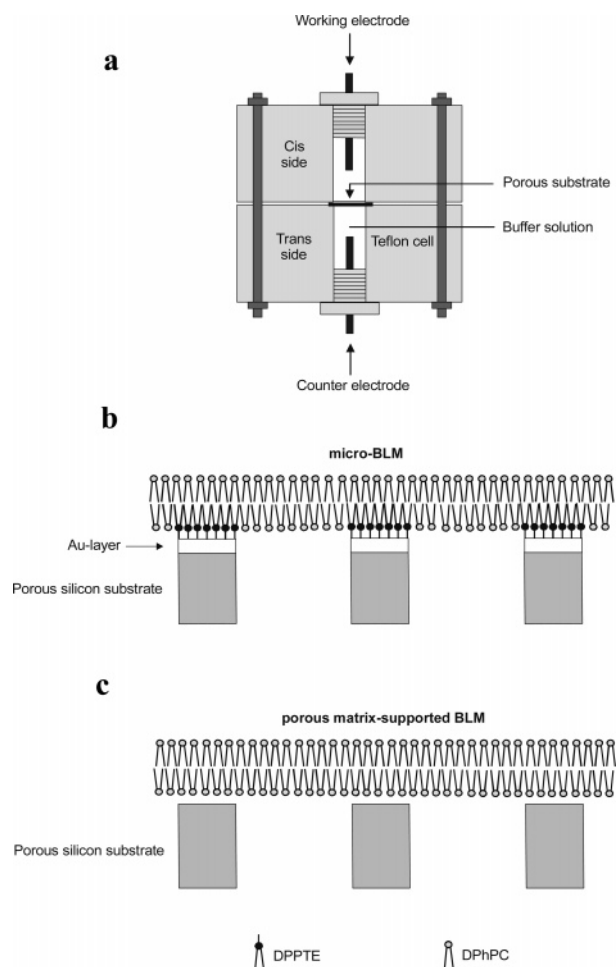


**Figure 2.** (a) Schematic drawing of the Teflon cell used for impedance analysis and single channel recordings. Platinum electrodes were used for impedance analysis, while Ag/AgCl electrodes were used for single channel recordings. (b) Schematic illustration of a micro-BLM composed of DPhPC and a DPPTE submonolayer chemisorbed on the gold-covered surface of the porous silicon substrate. (c) Representation of a porous matrix-supported BLM composed of DPhPC. The lipid bilayers supported on the macroporous silicon substrate are not drawn to scale.

Information). This indicates, as expected, that the current flows solely through the pores and that the silicon material itself does not influence the electrical behavior of the whole setup.

**Impedance Analysis of Micro- and Porous Matrix-Supported BLMs.** Two different preparation techniques were followed to form lipid bilayers suspending the highly ordered silicon macropore arrays with pore diameters of  $1.0 \pm 0.1 \mu\text{m}$ :

(i) In a first approach, the backside of the porous silicon was first coated with a thin gold layer, which allows for the chemisorption of the phospholipid 1,2-dipalmitoyl-*sn*-glycero-3-phosphothioethanol (DPPTE) rendering the surface hydrophobic. Both, the gold coating and the chemisorption of DPPTE do not alter the impedance behavior corroborating the idea that the current flows only through the pores. Second, the phospholipid 1,2-diphytanoyl-*sn*-glycero-3-phosphocholine (DPhPC) dissolved in *n*-decane was spread across the functionalized porous matrix (see Figure 2b). The formation of a lipid bilayer was followed by means of impedance spectroscopy in a frequency regime of  $10^{-2}$ – $10^6$  Hz using the setup depicted in Figure 2a. For very large membrane resistances impedance measurements down to  $10^{-3}$  Hz were carried out (see Supporting

Information). Electrical impedance spectroscopy enables one to obtain quantitative electrical parameters, which allow unambiguously distinguishing between single lipid bilayers and multilayers. Our measurements revealed the formation of single lipid bilayers consistent with a mean specific capacitance of  $0.6 \pm 0.2 \mu\text{F}/\text{cm}^2$ . The bilayer formation process takes about 10–20 min. During this time period, the initially formed hydrophobic lipid droplet with a thickness of several micrometers thins out to form a planar lipid bilayer completing the self-assembled DPPTE submonolayer, which can be followed by the increase in capacitance leveling off at the characteristic specific capacitance of a single lipid bilayer (see Supporting Information). Due to the similarity of this hybrid system to classical black lipid membranes and the fact that the bilayer suspends pores with diameters of  $1 \mu\text{m}$ , we termed these membranes micro-BLMs.

The membrane resistance  $R_m$  is determined in the very low-frequency regime. If  $R_m$  is larger than  $10 \text{ G}\Omega$ , it is not detectable in the observed frequency regime and is classified as  $R_m > 10 \text{ G}\Omega$ . Below  $10 \text{ G}\Omega$ , the parameter  $R_m$  of the equivalent circuit shown in Figure S1a (Supporting Information) was fitted to the data with a relative fitting error of  $< 10\%$ .

(ii) In a second approach suspended lipid bilayers were formed on macroporous silicon substrates without gold- and DPPTE-coating by simply spreading DPhPC in *n*-decane onto the porous matrix (see Figure 2c). Impedance spectra again clearly show the formation of an insulating lipid bilayer across the porous matrix characterized by a mean specific membrane capacitance of  $(0.8 \pm 0.3) \mu\text{F}/\text{cm}^2$ . Membrane resistances were again larger than  $10 \text{ G}\Omega$ . This membrane type is termed matrix-supported BLM.

**Long-Term Stability of Micro- and Matrix-Supported BLMs.** The membrane capacitances and resistances achieved for micro-BLMs and matrix-supported BLMs based on silicon macropores resemble those obtained for classical BLMs, and the membrane resistances are sufficiently high to perform single channel recordings (see below). However, for ion channel biosensors, not only the electrical characteristics but also the long-term stability of these parameters are of major importance. Classical BLMs typically rupture in one single event, leading to a complete loss of membrane resistance and capacitance. To investigate the behavior of micro-BLMs, the time course of the membrane capacitance and resistance has been investigated by means of impedance spectroscopy (Figure 3). One hour after membrane formation, the micro-BLM exhibits a resistance of  $> 10 \text{ G}\Omega$ . The value decreases over time, leading to a membrane resistance of  $5 \text{ G}\Omega$  after 24 h,  $2 \text{ G}\Omega$  after 50 h, and  $1.5 \text{ G}\Omega$  after 70 h. This indicates that only a limited area of the membrane suspending the pores ruptures, while other areas are still membrane-covered. This is corroborated by the capacitance measurements, which demonstrate that the capacitance of the micro-BLMs only slightly increases concomitant with the decrease in membrane resistance and the idea that the majority of the silicon substrate is then still covered by a membrane. In summary, a typical micro-BLM exhibits a membrane resistance of larger than  $1 \text{ G}\Omega$  for approximately 1 day. We simply defined  $1 \text{ G}\Omega$  as a threshold value, as this membrane resistance is sufficiently large to perform single channel recordings.

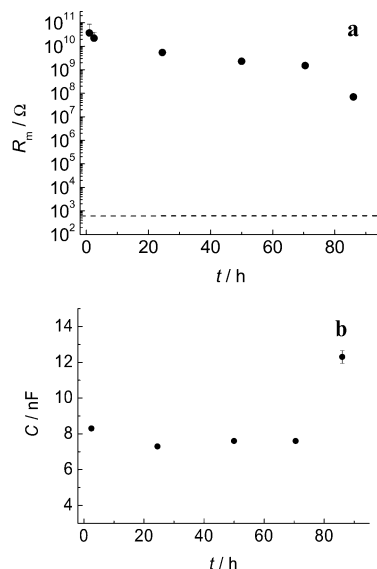


**Figure 3.** (a) Time course of the membrane resistance  $R_m$  and (b) the membrane capacitance  $C_m$  obtained by electrochemical impedance analysis of a micro-BLM in a frequency range of  $10^{-2}$ – $10^6$  Hz. The membrane resistances and capacitances were obtained by fitting the parameters of the equivalent circuit shown in Figure S1b (Supporting Information). For membrane resistances larger than  $10\text{ G}\Omega$ , the plotted values are given only as the lower limits. The dotted line shows the theoretical resistance that would be obtained if the membrane is completely ruptured and only the electrolyte resistance becomes visible.

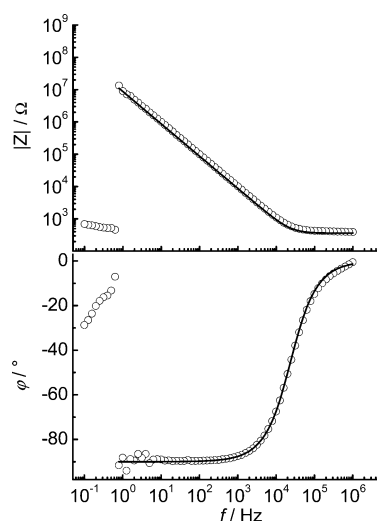


**Figure 4.** Impedance spectra of a porous matrix-supported BLM that ruptures during the time of the impedance recording. The solid line is the result of the fitting procedure with an equivalent circuit composed of a series connection of a capacitance  $C_m$  and a resistance  $R_{bs}$  in a frequency range of  $10^0$ – $10^6$  Hz.

The time-dependent change in membrane resistance  $R_m$  as a measure of long-term stability has also been investigated for matrix-supported BLMs. Although the achieved membrane resistances were in principle in the same range as those obtained for micro-BLMs, a continuous time-dependent decrease in membrane resistance was not observed. Instead, after a certain time, a complete loss in membrane resistance was monitored, indicative of a complete rupture of the membrane. Such an event was observed during the recording of an impedance spectrum (Figure 4), indicated by the sudden decrease of impedance, leading to a spectrum displaying only the resistance of the buffer solution. To verify that the membrane was still intact prior to

rupturing, part of the impedance spectrum that is characterized by the membrane capacitance  $C_m$  and the electrolyte solution ( $10^6$ – $10^0$  Hz) was taken to extract the exact value of the specific membrane capacitance. A value of  $1.05\ \mu\text{F}/\text{cm}^2$  was obtained, confirming the quality of the membrane before it ruptured. In general, membrane resistances for matrix-supported BLMs suited for single channel recordings were found within a broad time interval up to several hours.

In conclusion, only micro-BLMs exhibit the desired electrical and mechanical long-term stability for biosensor applications.

**Channel Activity of Synthetic Vpu<sub>1–32</sub> Peptide.** Micro-BLMs and matrix-supported BLMs, respectively, were subjected to an ion channel activity study of purified synthetic Vpu<sub>1–32</sub> comprising the transmembrane segment of Vpu. Micro-BLMs were utilized and the peptide dissolved in trifluoroethanol was added to the buffer solution of the *cis*-chamber after a stable baseline was monitored. Channel events were mostly observed shortly after peptide addition, indicating its insertion into the micro-BLM. Channel activity was observed for more than 15 individual bilayer preparations. The most frequently observed single channel openings of synthetic Vpu<sub>1–32</sub> displayed a conductance of  $12 \pm 3\text{ pS}$  in 5 mM HEPES, 0.5 M KCl, pH 7.4 and a less frequently observed one of  $28 \pm 3\text{ pS}$  (Figure 5a,b). Surprisingly, even 3 h after the first channel openings had been observed, distinct rectangular-shaped single channel events were discernible, with the most frequently observed at  $30 \pm 2\text{ pS}$  and the less frequently observed at the  $12 \pm 2\text{ pS}$  conductance state. Figure 5c,d shows representative opening states monitored around 1 h after the first channel events were observed.

Besides micro-BLMs, matrix-supported lipid bilayers were also used for single channel recordings to investigate the influence of the chemisorbed DPPTE monolayer of the micro-BLMs on Vpu channel activity. Again, peptide was added to the buffer solution, and channel events were detected shortly after peptide addition. First, current traces were observed, which indicate a single channel undergoing transitions between a closed (C) and two open (O) states at a holding potential of 50 mV (Figure 6a,b). Two discrete channel openings with a mean conductance of  $13 \pm 4\text{ pS}$  and  $25 \pm 2\text{ pS}$ , respectively, were observed occurring initially with almost equal frequency, but were considerably less frequently observed as the closed state. In contrast to the single channel recordings obtained for micro-BLMs, in case of porous matrix-supported BLMs already after a short incubation time, single channel events could not be resolved unambiguously anymore, but rather noisy current traces were recorded (Figure 6c).

#### Inhibition of Channel Activity by Amiloride Derivatives.

It has been shown that amiloride derivatives depress ion channel activity of full-length Vpu reconstituted in classical BLMs.<sup>22</sup> The binding site for the inhibitors has been suggested to be located in the N-terminal transmembrane domain of Vpu.<sup>28</sup> To prove if micro-BLMs are suited for the investigation of inhibitors of viral peptide channel activity, the influence of 5-(*N,N*-hexamethylene)amiloride (HMA), 5-(*N,N*-dimethyl)amiloride (DMA), and amiloride on the channel activity of Vpu reconstituted in micro-BLMs was investigated. The addition of an aqueous solution of HMA to the *cis*- and *trans*-chambers with a final concentration of  $100\ \mu\text{M}$  in each chamber resulted in

(28) Lemaitre, V.; Ali, R.; Kim, C. G.; Watts, A.; Fischer, W. B. *FEBS Lett.* **2004**, *563*, 75–81.

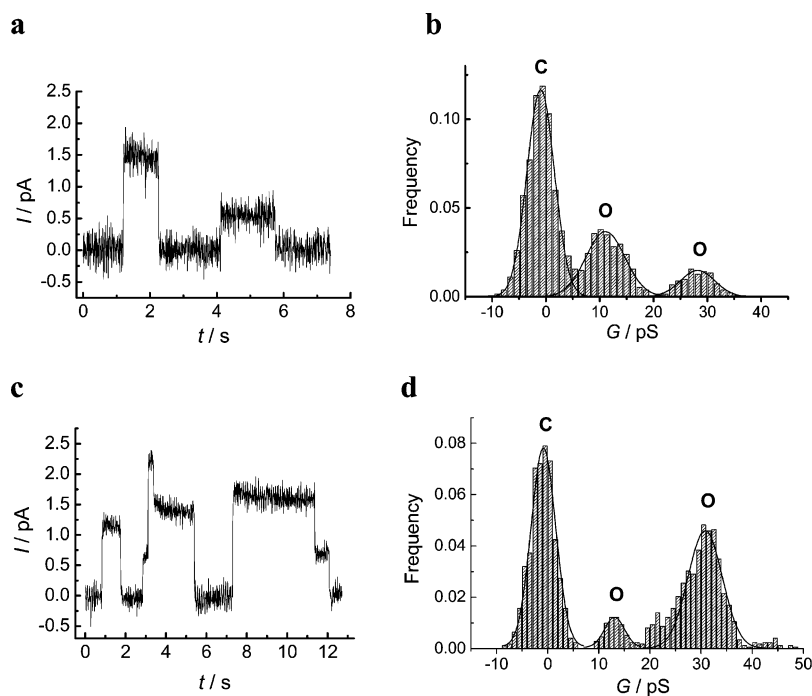


**Figure 5.** Channel recordings from synthetic transmembrane segments of Vpu reconstituted into micro-BLMs based on silicon macropores. Currents were recorded in symmetric buffer composed of 5 mM HEPES, 0.5 M KCl, pH 7.4. The solid line labeled with C indicates the current of the closed state, while O indicates that of the open states. (a) Segment of a continuous recording, observed shortly after peptide addition to the buffer solution. (b) Current histogram and Gaussian fit results obtained from continuous segments illustrating the occurrence of a 12 and 28 pS open channel state at a holding potential of 50 mV. (c) Current trace observed approximately 1 h after the first channel openings. (d) Current histogram displaying two main open channel states at 13 and 30 pS, respectively, at a holding potential of 50 mV.

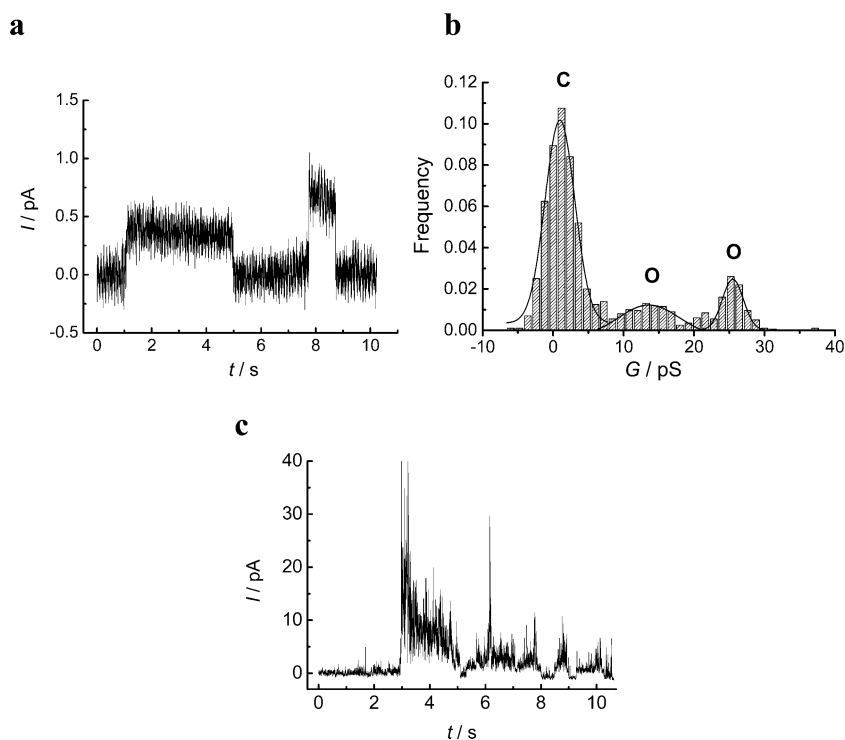


**Figure 6.** Channel recordings from synthetic transmembrane segments of Vpu reconstituted into matrix-supported BLMs based on silicon macropores. (a) A short current trace, recorded at a holding potential of 50 mV, was selected to illustrate the occurrence of single channel conductance, observed shortly after peptide addition to the buffer solution. (b) Current histogram and Gaussian fits revealing single channel events with conductance levels of 13 and 25 pS, respectively. (c) Current trace recorded about 10–20 min after the first channel events have been observed. This current pattern of channel activity reproducibly occurred shortly after the observation of the first single channel conductance.

complete inhibition of Vpu<sub>1-32</sub> single channel activity after approximately 10 min (see Supporting Information). Inhibition of single channel activity was also found for DMA within 10

min, while amiloride itself with a final concentration of 100  $\mu$ M in 5 mM HEPES, 0.5 M NaCl, pH 7.4 and a holding potential of 50 mV did not inhibit the channel activity of Vpu.

## Discussion

This work describes for the first time the development of micro-BLMs as a system well suited to the study of single ion channels formed by the N-terminal transmembrane domains of the viral protein Vpu<sub>1–32</sub> from HIV-1. Impedance analysis of the membranes unambiguously proved the formation of single lipid bilayers consistent with the mean specific capacitance of  $0.6 \pm 0.2 \mu\text{F}/\text{cm}^2$  that was also found for classical BLMs and nano-BLMs.<sup>2,29,30</sup> To observe single channel events with low noise, high membrane resistances in the  $G\Omega$  regime are required. Micro-BLMs exhibit membrane resistances larger than  $1 G\Omega$ , which are similar to those obtained for classical BLMs<sup>2</sup> and much larger than those typically obtained for solid-supported membranes.<sup>2,31</sup>

To establish a membrane system suited for biosensor devices and high-throughput screening systems based on single channel recordings, not only the membrane resistance itself but also a long-term stability of the membrane is required. The lifetime of a micro-BLM was defined here as the time period over which the membrane resistance exceeds  $1 G\Omega$ . On the basis of this definition, a mean lifetime of around 1 day was obtained. The most striking difference between classical BLMs, porous matrix-supported BLMs, and micro-BLMs was the finding that in the case of micro-BLMs the membrane resistance decreases with time. For conventional BLMs<sup>2</sup> spanning a small hole in a thin Teflon film, and for those bilayers more recently described and formed on individual apertures manufactured in silicon or glass supports,<sup>9,12</sup> the membrane always ruptures in one single step, which can be deduced from the measured low resistance of several hundred  $\Omega$ . Stabilities of conventional BLMs with pore diameters of  $0.1–1 \text{ mm}$  are reported to be typically in the range of several hours.<sup>2</sup> Schmidt et al.<sup>9</sup> reported a membrane suspending a  $0.6–7 \mu\text{m}$  hole in silicon, which ruptures approximately after 1 h, whereas Cheng et al.<sup>12</sup> obtained a stability of 5 h for a lipid bilayer suspended across an orifice of  $128 \mu\text{m}$  in diameter before it completely ruptured. The notion that micro-BLMs do not rupture in one single step indicates that only membrane patches rupture that do not influence the stability of the entire membrane. This significantly different behavior of the membrane resistance of micro-BLMs and porous matrix-supported BLMs led us to conclude that the immobilization of the lipid bilayer on the porous silicon matrix via DPTE chemisorbed on the pore rims decouples the free-standing membranes from each other.

Despite this difference in long-term stability and rupture mechanism, both membrane types, micro-BLMs as well as porous matrix-supported BLMs, allow in principle single channel recordings. Here, the suitability of micro-BLMs has been demonstrated by investigating the channel activity of the synthetic peptide Vpu<sub>1–32</sub>. Over the past years it has been established that the transmembrane  $\alpha$ -helix (residues 8–25) of the Vpu polypeptide exhibits ion channel activity. All that data were acquired from single channel recordings on classical planar lipid bilayers after reconstitution of full-length Vpu or truncated versions (Vpu<sub>1–27</sub>, Vpu<sub>2–30+</sub>, Vpu<sub>2–37</sub>, Vpu<sub>2–51</sub>) of the protein.<sup>18–26,32,33</sup> By means of the newly established micro-BLM

system, single and multichannel openings of heterogeneous conductance in a highly resolved manner were recorded. The most frequent conductance state of  $12 \text{ pS}$  in  $5 \text{ mM}$  Hepes,  $0.5 \text{ M}$  KCl, pH 7.4 was largely observed as distinct single channel openings similar to the observation of Ma et al.<sup>33</sup> They reported a single channel conductance of  $12 \pm 2 \text{ pS}$  as the most frequently observed opening for Vpu<sub>2–37</sub> under similar conditions using classical BLMs. The conductance level of  $12 \text{ pS}$  is also consistent with experiments carried out by Marassi et al.<sup>18</sup> using full length Vpu and Vpu<sub>2–51</sub> and Ewart et al.<sup>22</sup> using Vpu constructs including the transmembrane domain. The observed  $12 \text{ pS}$  conductance state is also observed for full-length Vpu, with the most frequently occurring conductance of  $12, 22,^{18,26}$  and  $30 \text{ pS}^{20}$  recorded in  $0.5 \text{ M}$  KCl. The finding that the second single channel conductance of  $28 \text{ pS}$  becomes more prominent after some time is consistent with the observations of Schubert et al. (Vpu<sub>1–27</sub>)<sup>21</sup> and Marassi et al.<sup>18</sup> using full length Vpu and Vpu<sub>2–51</sub> and Kochendoerfer et al.<sup>20</sup> (full length Vpu).

The results obtained for Vpu channel activity highlight that micro-BLMs are suited for single channel studies. They show advantages over classical BLMs, lipid bilayers suspending micromachined apertures, and porous matrix-supported BLMs. Using micro-BLMs, different single channel conductance states were resolved even 3 h after peptide had been added to the aqueous phase. In contrast, in the case of porous matrix-supported BLMs, single channel events could be observed only within the first 10–20 min. Already 10–20 min after peptide addition, large current bursts become visible, whose magnitudes increase over time presumably due to an increased number of inserted Vpu peptides. Such large conductance bursts of up to  $430 \text{ pS}$  were also reported by Ewart et al.<sup>22,24</sup> using classical BLMs and were attributed to many simultaneously opened channels or the association of a large number of Vpu monomers to large channel aggregates, respectively. From our results we hypothesize that the chemisorbed DPTE monolayer anchoring part of the micro-BLM to the support might reduce the lateral mobility of the lipids and thus influences the lateral mobility of incorporated Vpu monomers. This would result in a slower rate of assembly of large oligomeric bundles of Vpu monomers, and as a consequence, multichannel bursts due to oligomerization by large conducting channel aggregates as observed in matrix-supported BLMs become less probable within the observed time period. In addition, it is also conceivable that the incorporation probability of peptides is reduced due to the DPTE-immobilized hybrid lipid bilayer, also resulting in less frequently observed multichannel bursts.

Although the hindrance of large channels is particularly advantageous for the investigation of Vpu, this phenomenon may be disadvantageous for other diffusion-controlled channel-forming compounds. If the insertion probability is less and the lateral mobility of the lipids and channel-forming compounds is reduced, this would disfavor the channel formation process, and hence, the observation of single channel events becomes less likely in micro-BLMs, while it might still be observable in classical or matrix-supported BLMs.

(29) Benz, R.; Fröhlich, O.; Lauger, P.; Montal, M. *Biochim. Biophys. Acta* **1975**, *394*, 323–334.

(30) Römer, W.; Steinem, C. *Biophys. J.* **2004**, *86*, 955–965.

(31) Terretaz, S.; Mayer, M.; Vogel, H. *Langmuir* **2003**, *19*, 5567–5569.

(32) Cordes, F. S.; Tustian, A. D.; Sansom, M. S.; Watts, A.; Fischer, W. B. *Biochemistry* **2002**, *41*, 7359–7365.

(33) Ma, C.; Marassi, F. M.; Jones, D. H.; Straus, S. K.; Bour, S.; Strelbel, K.; Schubert, U.; Oblatt-Montal, M.; Montal, M.; Opella, S. J. *Protein Sci.* **2002**, *11*, 546–557.

## Experimental Section

**Materials.** (100) *n*-type silicon wafers with a resistivity of 0.5  $\Omega\text{cm}$  were supplied from Wacker (Germany). Hydrofluoric acid p.a. (40%) was purchased from Merck (Darmstadt, Germany). 1,2-Diphytanoyl-*sn*-glycero-3-phosphocholine (DPhPC) and 1,2-dipalmitoyl-*sn*-glycero-3-phosphothioethanol (DPSTE) were obtained from Avanti Polar Lipids (Alabaster, AL). The peptide Vpu<sub>1-32</sub> corresponds to the N-terminal 32 amino acids of Vpu, with the sequence MQPIPIVAIV<sup>10</sup> ALVVAII-IAI<sup>20</sup> VVWSIVIIIEY<sup>30</sup> RK (molecular weight: 3544 g/mol).<sup>32</sup> It was synthesized on a Pioneer Synthesizer from Applied Biosystems Instruments using Fmoc-chemistry. Purification was achieved using a Gilson HPLC system with a C18 reversed-phase column. 5-(*N,N*-Hexamethylene)amiloride (HMA), 5-(*N,N*-dimethyl)amiloride, and amiloride were purchased from Sigma-Aldrich (Taufkirchen, Germany) and stored in the dark. The water used was ion-exchanged and Millipore-filtered (Millipore Milli-Q-System, Molsheim, France, specific resistance  $R > 18 \text{ M}\Omega \text{ cm}^{-1}$ , pH 5.5).

**Preparation of Macroporous Silicon Substrates.** Highly ordered silicon macropore arrays with pore diameters of 1  $\mu\text{m}$  were produced using photolithography followed by anodization in hydrofluoric acid. First, pore nuclei (initiation spots) are defined on the (100) *n*-type silicon wafer by standard photolithography.<sup>34</sup> Second, the pore nuclei are extended to inverted pyramids by an alkaline etch. Third, cylindrical macropores are grown starting from the pore nuclei by photoelectrochemical anodization in HF ( $c_{\text{HF}} = 4 \text{ wt } \%$ ;  $T = 10 \text{ }^\circ\text{C}$ ;  $U = 2.7 \text{ V}$ ). The silicon wafer is inserted in an anodization chamber with its front side exposed to aqueous HF, while the backside is illuminated by light to generate electronic holes in the valence band of silicon. The sample is anodically biased by a transparent backside ohmic contact. A platinum wire immersed in the HF solution serves as cathode. During the anodization process, holes diffuse from the wafer backside to the etch front and are consumed at the pore tips. This promotes the dissolution of the silicon almost exclusively at the pore tips due to the enhanced electrical field in the space charge layer, leading to further pore growth perpendicular to the (100) surface with very high aspect ratio.

A porous silicon structure with continuous open pores is created by selective dissolution of the backside of the nonporous silicon wafer. After the electrochemical anodization process, a protective SiO<sub>2</sub> film of about 30 nm covering the entire silicon structure is formed by thermal oxidation at 800  $^\circ\text{C}$  in an oxygen atmosphere for 3 h. The SiO<sub>2</sub> layer is then selectively removed from the backside of the silicon wafer by HF, and the silicon dissolved by an anisotropic KOH etching process in 25 wt % KOH at 90  $^\circ\text{C}$ . SiO<sub>2</sub> at the pore walls acts as an etch stop for KOH. After this procedure, the pore bottoms are still covered with SiO<sub>2</sub>. A second HF dip removes the SiO<sub>2</sub> from the backside and opens the pores. A native hydrophilic SiO<sub>2</sub> layer is then formed on the silicon-covered hydrophobic pore rims of the backside upon incubation in aqueous solution.

### Formation of Micro-BLMs and Porous Matrix-Supported BLMs.

For micro-BLMs, the bottom surface of the macroporous silicon is first coated with a 100 nm gold layer using a sputter coater with a thickness control unit (Cressington sputter coater 108auto, Cressington MTM-20, Elektronen-Optik-Service, Dortmund, Germany). Selective functionalization of the gold surface is then achieved by chemisorption of DPSTE for at least 12 h from a 0.5 mM ethanolic DPSTE solution. After thoroughly rinsing with ethanol and drying under a stream of nitrogen the porous substrate is horizontally placed in the Teflon chamber (see Figure 2a), acting as a diaphragm that separates the *cis* from the *trans* compartment. Subsequently, both compartments are filled with buffer solution. Lipid bilayers are accomplished by painting 10  $\mu\text{L}$  of DPhPC dissolved in *n*-decane (1% (w/v)) across the hydrophobic DPSTE-covered backside of the porous silicon substrate.

For porous matrix-supported BLMs, the backside of the substrate is not coated with gold and selectively functionalized. Instead, lipid

bilayers are directly prepared by painting 10  $\mu\text{L}$  of DPhPC dissolved in *n*-decane (1% (w/v)) across the backside of the hydrophilic SiO<sub>2</sub>-coated porous silicon substrate.

**Electrochemical Impedance Spectroscopy.** Porous silicon substrates with and without lipid bilayers are investigated by means of electrical impedance spectroscopy. AC impedance spectroscopy is performed using the impedance gain/phase analyzer SI 1260 and the 1296 Dielectric Interface (Solartron Instruments, Farnborough, UK) controlled by a personal computer. A small sinusoidal ac voltage of 30 mV is applied to the system at zero offset potential, and the current response is measured in terms of absolute values of the complex impedance  $|Z|(f)$  and phase shift  $\varphi(f)$  between voltage and current within a frequency range of  $10^{-3}/10^{-2}$ – $10^6$  Hz. Impedance data are recorded with the Solartron Impedance Measurement Software (Version 3.5.0) as equally spaced data points (five data points per decade) on a logarithmic scale and analyzed using the software package ZView2.6b with Calc-Modulus data weighting. For data presentation, Bode plots of  $|Z|(f)$  and  $\varphi(f)$  as a function of frequency are displayed.

Electrochemical measurements were carried out using the Teflon cell schematically depicted in Figure 2a. The cell consists of two identical compartments each with a volume of 4 mL "separated" by the porous silicon substrate with an area of  $A = 7 \text{ mm}^2$  sealed by an O-ring. Platinum wires immersed in the buffer solution on both sides are connected with the impedance analyzer and serve as working (*cis* compartment) and counter electrode (*trans* compartment).

**Single Channel Recordings.** Channel recordings are conducted in the Teflon cell (Figure 2a). Electrical currents are recorded with an Axopatch 200B patch clamp amplifier (Axon Instruments, Foster City, CA) in capacitive feedback configuration via Ag/AgCl electrodes. The electrode of the *cis* compartment is connected to ground. Single channel currents were all recorded at an applied voltage of 50 mV. Data were filtered at 1 kHz with an 8-pole Bessel filter, and the analogue output signal was digitized at a sampling rate of 5 kHz by using an A/D converter (Digidata 1322A, Axon Instruments). Data processing is performed using pClamp 8.0 software (Axon Instruments). To avoid electrostatic interference during measurements, the electrochemical cell is placed in a Faraday cage set on a mechanically isolated support.<sup>35</sup>

Single channel experiments are carried out in symmetrically buffered solutions composed of 5 mM Hepes and 0.5 M KCl, pH 7.4 at room temperature. After formation of stable lipid bilayers, Vpu<sub>1-32</sub> is added to the *cis* compartment from a  $10^{-6}$  M stock solution in trifluoroethanol, leading to a final concentration of approximately  $10^{-9}$  M. The illustrated channel current recordings are representative of the most frequently observed conductance under the applied experimental conditions. Single channel conductance was calculated from the corresponding Gaussian fits to current histograms by using data from segments of continuous recordings lasting longer than 10 s. Openings shorter than 0.5 ms were ignored.

## Conclusions

A planar chip-based arrangement of so-called micro-BLMs with resistances larger than 1 G $\Omega$  based on highly ordered macroporous silicon arrays, which are on average stable for 1 day, has been designed, which is the crucial step toward an automated and paralleled array for ion channel recordings that will pave the way for ion channel screening assays.

**Acknowledgment.** This work was supported by the Bundesministerium für Bildung und Forschung within the nanobio-technology project. We thank S. Schweizer for technical support. W.B.F. and A.W. thank the E. P. Abraham Research Fund, the Medical Research Council (MRC), and the Bionanotechnology

(34) Müller, F.; Birner, A.; Gösele, U.; Lehmann, U.; Ottow, S.; Föll, H. J. *Porous Mater.* **2000**, *7*, 201–204.

(35) Hanke, W.; Schlue, W. R. *Planar lipid bilayers: methods and applications*; Academic Press: London, 1993.



IRC for financial support. The Fonds der Chemischen Industrie is gratefully acknowledged for financial support.

**Supporting Information Available:** Impedance spectra, time-resolved change in capacitance during micro-BLM formation,

and current traces before and after addition of HMA. This material is available free of charge via the Internet at <http://pubs.acs.org>.

JA0451970